TOXICOLOGICAL SCIENCES **122(2)**, 395–405 (2011)
doi:10.1093/toxsci/kfr131
Advance Access publication May 20, 2011

Transmembrane Transport of Microcystin to *Danio rerio* Zygotes: Insights into the Developmental Toxicity of Environmental Contaminants

Chao Song, Hong-Wen Gao,[1] and Ling-Ling Wu

State Key Laboratory of Pollution Control and Resources Reuse, College of Environmental Science and Engineering, Tongji University, Shanghai, 200092, China

[1]To whom correspondence should be addressed. Fax: (+86) 21-6598-8598. E-mail: EMSL@tongji.edu.cn.

Received February 3, 2011; accepted May 13, 2011

Microcystins (MCs) produced by cyanobacteria and their continuing "blooms" are a worldwide problem owing to the toxicity of microcystin-LR (MC-LR) to plants and animals. In the present study, we investigated membrane transport of MC-LR and its toxic effects on zebrafish embryos using fragmentation of embryos, scanning electron microscope (SEM), fluorescence microscopy, and toxic exposure tests. At a concentration < 0.04 mmol/l, MC-LR was predominantly adsorbed on outer membrane surface of embryos according to Langmuir isotherm. The absorption characteristics of MC-LR within the range from 0.05 to 0.4 mmol/l conformed to Freundlich isotherm model. At concentrations > 0.50 mmol/l MC-LR directly entered the cytoplasm via partition. Thinning and disruption of membranes was confirmed using SEM and fluorescence morphological observations. Exposure to different concentrations of MC-LR resulted in differences in membrane transport and toxicity characteristics. At low concentrations, more than 75% of the adsorbed MC-LR accumulated on the outer membrane surface and resulted in axial malformation, tail curving, and tail twisting. Increasing the concentration of MC-LR to between 0.05 and 0.4 mmol/l improved membrane transport and it was evident in cytoplasm of embryos, resulting in serious pericardial edema, hatching gland edema, hemagglutination, hemorrhage, and vacuolization. At > 0.50 mmol/l, more than 70% of the adsorbed MC-LR entered the cytoplasm and this was lethal to the embryos. The current research outlines a new method and mechanism for the transmembrane transport of large molecular weight organic compounds and could be important for studies concerning molecular toxicology.

Key Words: **transmembrane transport; microcystin-LR; zebrafish; developmental toxicity.**

Microcystins (MCs) are cyclic nonribosomal peptides produced by several species of cyanobacteria including those belonging to the genera *Microcystis*, *Anabaena*, and *Planktothrix* (Djediat *et al.*, 2010). MCs contains several uncommon nonproteinogenic amino acids including dehydroalanine derivatives and the β-amino acid (*all-S*, *all-E*)-3-amino-9-methoxy-2, 6, 8-trimethyl-10-phenyldeca-4,6-diene acid (ADDA). More than 80 MCs have been successfully isolated and identified. Microcystin-LR (MC-LR) is the most abundant and most toxic worldwide (Fastner *et al.*, 2002), leading to investigations by chemists, pharmacologists, biologists, and ecologists from all over the world. The majority of studies concerning MC-LR have demonstrated its toxicity toward plants and animals, and it is recognized as an inducer of potent environmental stress in aquatic ecosystems and as a potential threat to human health (Miller *et al.*, 2010; Stone and Bress, 2007). MCs derived from continuing "blooms" constitute a worldwide problem affecting several countries including China, Brazil, Australia, the United States, and much of Europe. Once MCs are ingested, most travel to the liver via the bile acid transport system and are stored. However, some remain in the blood stream and can contaminate various tissues. MCs bind covalently to protein phosphatases and disrupt cellular control processes. MC-LR strongly inhibits protein phosphatase type 1(PP1) and protein phosphatase type 2A (PP2A) (Hastie *et al.*, 2005; Malbrouck *et al.*, 2004; Tachi *et al.*, 2007) and demonstrates tumor-promoting activity (Gan *et al.*, 2010). A few studies have suggested a relationship between liver and colorectal cancers and the occurrence of cyanobacteria in drinking water (Zhou *et al.*, 2002). However, there is insufficient information to assess the carcinogenic potential of MCs applying Environmental Protection Administration Guidelines for Carcinogen Risk Assessment. Several studies have demonstrated that the mechanism underlying an agent's toxicity is related to its membrane interactions (Donato *et al.*, 1997a; Lopes *et al.*, 1997; Sikkema *et al.*, 1995). The present study confirms that the toxic mechanism of an agent is related to membrane interactions but also concludes that it is related to the type of membrane transport it undergoes (Fei *et al.*, 2010; Song *et al.*, 2010). In previous studies, *Bacillus stearothermophilus* was chosen as the model system for assessing the toxicity of several lipophilic environmental pollutants including endosulfan, dichlorodiphenyltrichloroethane, and tamoxifen (Donato *et al.*, 1997b; Martins *et al.*, 2003; Monteiro *et al.*, 2003). In the present study, zebrafish embryos were chosen as the model system to investigate lipophilic and

hydrophilic environmental pollutants. The pollutants investigated in previous studies are relatively simple in terms of structure and polarity. MC-LR has a more complex structure, containing hydrophobic groups in addition to hydrophilic groups.

Several recent reports concern early life-stage toxicity (ELS) effects of MC-LR (Fischer and Dietrich, 2000; Huynh-Delerme *et al*., 2005; Jacquet *et al*., 2004). Previous studies have elucidated toxicity-causing mechanisms underlying exogenous chemicals by focusing on interactions with target molecules *in vitro* (Li *et al*., 2010; Zhang *et al*., 2010), protein expression (Jayaraj *et al*., 2006; Mezhoud *et al*., 2008), alteration of gene sequences (Li *et al*., 2009; Schwarzenberger *et al*., 2009), and dose-effect relationships (Herfindal and Selheim, 2006; Wang *et al*., 2005). However, chemicals that affect the function of a target biomolecule having penetrated the cell must have interacted with the cell membrane before inducing toxicity (Li *et al*., 2007). The limited information concerning the mechanisms underlying the toxicity of MC-LR may be due to a lack of understanding its interactions with the membrane and the membrane transport process to which it is subject. Zebrafish are an ideal model for investigating developmental toxicity in vertebrates during ELS (Lahnsteiner, 2008; Nagel, 2002). Therefore, embryos were exposed to MC-LR, a representative of MCs. The aim of this study was to understand the developmental toxicity caused by MC-LR and elucidation of associated membrane transport pathways.

MATERIALS AND METHODS

Apparatus and materials. A high-performance liquid chromatography (HPLC) (Model L-2000, Hitachi, Japan) with an L-2130 pump, a diode array detector (DAD) (Model L-2455), and an inverse-phase column (C18, Model Eclipse Plus 5 μm 4.6 × 150 mm; Agilent) was used to determine the concentration of MC-LR. A freeze-dryer (Model K750X; Jintan Etong Electrons, China) was used to prepare freeze-dried embryos for morphology of the outer membrane surface using the scanning electron microscope (SEM) (Model S-4800; Hitachi Inc., Japan). An ultrasonic cleaner (the bath sonicator, Model SK3300HP; Shanghai KUDOS ultrasonic Instruments, China) was used to disperse the lecithin and remove MC-LR from the outer membrane surface. An ultrasonic cell disruptor (the probe-type sonicator, Model JY92-II; Ningbo Scientz Biotechnology Co., Ltd, China) was used to prepare the liposome, disrupt the embryos, and break membrane. A high-speed centrifuge (Model TGL-16M; Changsha Xiangyi Centrifuge Instrument Co., Ltd, China) was used to separate MC-LR from the suspension after sonication. An inverted microscope (Model TE2000-U; Nikon, Inc., Japan) with 100 w high-pressure mercury lamp excitation and with B, G, UV fluorescence filter blocks (Nikon), a charge-coupled device (Evolution MP; Media Cybernetics, Japan), and digital photomicrography computer software (Image-Pro *Plus* 6.0) was used to observe toxicity-related changes in zebrafish embryos and larvae.

MC-LR (CAS 101043-37-2, Product code GE-LR-001, 95–99% by HPLC) was obtained from Shanghai Green Emperor Environmental Protection S&T Co., Ltd, China. Trifluoroacetic acid (CAS 76-05-1 and Lot No.802231) was purchased from Tedia Company, Inc. Methanol (CAS 67-56-1 and Product No.1060074000) was obtained from Merck KGaA (Germany). Green fluorescent cell membrane probe (DiO, CAS 34215-57-1) was purchased from Beyotime Institute of Biotechnology (China). Britton-Robinson buffers at pH 2.5, 3.5, 4.5, 5.5, 6.5, and 7.5 were prepared to investigate the pH effects and NaCl concentrations from 0.05 to 0.25 mol/l used to examine the effects of electrolytes at different temperatures ranging from 15°C to 55°C. Reconstituted buffer (ISO 6341) was prepared by mixing 0.294 g of $CaCl_2{\cdot}2H_2O$, 0.123 g of $MgSO_4{\cdot}7H_2O$, 0.065 g of $NaHCO_3$, and 0.006 g of KCl in 1 l of deionized water. A stock solution of MC-LR (4 mmol/l) was prepared in deionized water and diluted daily to the desired concentrations. A calibration curve of MC-LR was prepared by measuring the absorption peak area of MC-LR at 238 nm using an HPLC-DAD (see Supplementary 2, Fig. S1). The MC-LR concentration was calculated from the calibration curve. All organic solvents were HPLC grade.

Preparation of liposomes. Lecithin (CAS 8002-43-5, Product No. 69014933) was obtained from Sinopharm Chemical Reagents (China). The components of the lecithin was quantitatively analyzed by HPLC with an evaporative light scattering detector (ELSD-UM3000; Tianjin Watson Analytical Instruments Co., Ltd, China) using a normal phase column (Luna 5 μ Silica (2) 100 Å, 5 μm, 250 × 4.60 mm; Phenomenex), which contained phosphatidylcholine (PC, 95.4%), phosphatidylethanolamine (3.0%), and palmitic acid triglyceride (1.6%) in weight (Song *et al*., 2010). The lecithin was suspended in deionized water at a concentration of 20 g/l and ultrasonicated for 300 s at 0°C using a bath sonicator (SK3300HP) with the intervals of 30 s for sonication and 30 s for rest. Single-membrane liposomes (SML) were obtained by ultrasonicating for 300 s at 4 °C using a probe-type sonicator (JY92-II) at 120 w with the intervals of 15 s for sonication and 45 s for rest under a constant stream of nitrogen (Sikkema *et al*., 1994). The lecithin was extracted from the organism of egg yolk, and the vast majority components in lecithin is PC, which occurs in all cellular organisms, being one of the major components of the phospholipid portion of the cell membrane. SML prepared by PC showed the similar structure and properties with the natural membrane, so SML can be used to simulate the biological membranes.

Adsorption of MC-LR on SML. MC-LR was mixed with SML in 1.0 ml of deionized water, where the concentrations of MC-LR ranged from 0.016 to 3.5 mmol/l and that of PC in SML remained at 4 mmol/l. The mixture was incubated for 4 h and centrifuged for 10 min at 2012 × g. The concentration of MC-LR in the supernatants was determined by HPLC-DAD. Chromatographic conditions for determining MC-LR were as follows: the optimized mobile phase was water-methanol (34:66 vol/vol) with 1.25% trifluoroacetic acid in water (vol/vol), the flow rate was 1.0 ml/min (isocratic mode), the column temperature was 25°C, and the measurement wavelength was 238 nm. All injections (20.0 μl) were performed manually and MC-LR was eluted at 5.6 min (see Supplementary 2, Fig. S1). Each test was replicated three times.

Cultivation, collection, and exposure of embryos. The parental zebrafish were kept in a 25-l rectangular tempered glass tank (50 × 25 × 20 cm). The control settings of the water in the tank: The water (20 l) was ventilated for 24 h with an aquarium air pump (AP-45R, 3 l/min × 2; Guangdong Chuang Xing Electric Co., Ltd, China) to get 100% oxygen saturation (10.5 ± 0.5 mg/l) at room temperature. Then the water was heated for 30 min with the aquarium glass heater (AT-180; Guangdong Chuang Xing Electric Co., Ltd). Its temperature was maintained at 26.0°C ± 0.2°C and the saturation dissolved oxygen at 8.25 ± 0.4 mg/l. The water with the dissolved oxygen of 8.25 ± 0.4 mg/l, temperature of 26.0°C ± 0.2°C, pH of 7.5 ± 0.5, and hardness of 250 mg/l was used for rearing of the parental zebrafish. The dissolved oxygen in the water was monitored twice daily (8:00 A.M. and 20:00 P.M.) with a portable multiparameter meter (HQ40d; HACH Company). The light illumination was provided with the white fluorescent lights (T4, 10000K; Nanjing HAINENG Electric Light Source Co., Ltd, China) of 640 lx both at the surface of the water and the bottom of the tank. The photoperiod was controlled with a 24-h programmable timer (RS-03; Shanghai HAISHEN Plastic Electrical Appliance Co., Ltd, China) with the light/dark cycle of 14 h/10 h. The parental zebrafish were fed regularly with the frozen red mosquito larvae (Guangdong Shenzhen GONGLIN Co., Ltd, China) from an uncontaminated source twice daily (9:00 A.M. and 5:00 P.M.). On the evening before spawning was required, several rectangular spawning boxes (12 × 20 × 12 cm, DAZS 008-L; Sze Sun Aquarium & Pet Co., Ltd, Hong Kong, China) each containing six male and three female broodstock and a mesh (3–4 mm gap) were placed in the tank. Spawning was triggered once the light was turned on and was completed

within 30 min. The eggs were laid at the bottom of the spawning boxes with the depth of 6 cm. The fertilized eggs were collected and rinsed with reconstituted buffer (ISO 6341), which has been ventilated for 8 h to 10 l of water with the air pump (AP-45R) to get the dissolved oxygen of 8.18 mg/l (99.2% oxygen saturation) at 26°C. To ensure that the experiments produced valid results, normal embryos were screened with an inverted microscope (TE2000-U) and the fertilized eggs were obtained only from spawns with a fertilization rate of higher than 95%. Two hours postfertilization embryos and 2 h posthatching larvae were used in all the exposure experiments.

Fragmentation of embryos, extraction, and determination of MC-LR. In the membrane transport experiments, embryos were exposed to different concentrations of MC-LR solutions from 0.008 to 1.3 mmol/l, where 10 embryos were incubated in 1.0 ml of each solution for 36 h (see Supplementary 2, Fig. S2-1). The concentration (c_{L1}) of excess MC-LR in the supernatants was determined by HPLC-DAD (see Supplementary 2, Fig. S2-2). The exposed embryos (1) were isolated from the exposure solution (see Supplementary 2, Fig. S2-3) and (2) were suspended with 1.0 ml of deionized water (see Supplementary 2, Fig. S2-4). The suspended embryos (3) were ultrasonicated using the above bath sonicator for 90 s at 0°C with the intervals of 10 s for sonication and 5 s for rest (see Supplementary 2, Fig. S2-5). The MC-LR adsorbed on the outer membrane surface was dissolved into the suspension and its concentration (c_{L2}) was determined by HPLC-DAD (see Supplementary 2, Fig. S2-6). The treated embryos were (1) isolated from the suspension solution (see Supplementary 2, Fig. S2-7), (2) resuspended with 1.0 ml of deionized water (see Supplementary 2, Fig. S2-8), and then (3) ultrasonicated for 90 s at 0°C using the above probe-type sonicator at 120 w with the intervals of 10 s for sonication and 5 s for rest (see Supplementary 2, Fig. S2-9). The mixture was (4) filtered using the stainless steel filter with the aperture of 0.54 mm (30 mesh/inch; Dongguan Hongyuan Hardware Mesh Co., Ltd, China) to separate the membrane and cytoplasm. The membrane trapped on the filter was transferred to an Eppendorf tube (1.5 ml) and suspended with 1 ml of deionized water (see Supplementary 2, Fig. S2-10). The Eppendorf tube with the membrane suspension was (5) placed in a boiling water bath for 3 min (see Supplementary 2, Fig. S2-11). Then the Eppendorf tube was removed from the boiling water, cooled in ice, and ultrasonicated for 900 s (3) with the above probe-type sonicator at 240 w, with the intervals of 30 s for sonication and 15 s for rest (see Supplementary 2, Fig. S2-12). The mixture was (6) centrifuged for 5 min at 4°C at 2012 × g and the MC-LR in the membrane dispersed to the supernatant ($L_{3\text{-}1}$) (see Supplementary 2, Fig. S2-13). The residue (see Supplementary 2, Fig. S2-14) was resuspended (2) with 1 ml of 80% (vol/vol) methanol (see Supplementary 2, Fig. S2-15) and ultrasonicated (3) for 450 s by the same method above (see Supplementary 2, Fig. S2-16). The mixture was centrifuged (6) for 10 min at 4°C at 3578 × g, and the MC-LR in the residue of membrane was dispersed to the supernatant ($L_{3\text{-}2}$) (see Supplementary 2, Fig. S2-17). The supernatants from $L_{3\text{-}1}$ and $L_{3\text{-}2}$ were (7) mixed together and filtrated through 0.45 μm of microfiltration membrane, and (8) evaporated to 200 μl in a 40°C water bath. Then the concentration of MC-LR (c_{L3}) distributed inside of membrane was determined by HPLC-DAD (see Supplementary 2, Fig. S2-19). After filtration (4) of the mixture of membrane and cytoplasm, the cytoplasm was dispersed in the filtrate (see Supplementary 2 Fig. S2-20) and the MC-LR distributed in the cytoplasm (c_{L4}) extracted and determined (see Supplementary 2 from Fig. S2-21 to Fig. S2-29) by the same methods (see Supplementary 2 from Fig. S2-11 to Fig. S2-19). Therefore, the concentrations of MC-LR in different parts of embryos, that is, extracellular solutions (c_{L1}), outside (c_{L2}) and inside (c_{L3}) of the membrane and cytoplasm (c_{L4}), were determined and their q_e calculated. At the same time, the blank control was cultured in the reconstituted buffer (ISO 6341), which was administered by the same methods as that the above experimental group. The positive control was employed by adding a known concentration of MC-LR in the blank control at each step to evaluate the recovery of MC-LR in different parts of embryo during the extraction process. Each test was replicated three times. The recovery of MC-LR in outside and inside of the membrane and cytoplasm was calculated to be 94.5, 92.5, and 93.4%.

SEM and fluorescent morphology of the embryo membrane surface. Ten embryos were exposed to 0, 0.01, 0.10, and 1.00 mmol/l MC-LR, respectively. After incubation for 12 h, the supernatant was removed, and the embryos were freeze-dried for 12 h at −55°C. The SEM morphology of the lyophilized embryos was observed using SEM, and photographs were captured. After incubation for 12 h, each supernatant was removed, and the embryos were incubated with 10μM DiO for 10 min. The morphology of the exposed embryos was observed using an inverted microscope (TE2000-U). Photographs were captured and differences observed and noted.

Toxicological test of MC-LR with embryos and larvae. Ten embryos (10 larvae) were exposed to MC-LR solutions (10.0 ml) in semi-static conditions (24 h renewal), and 25-ml glass petri dishes were used as test chambers. The test chambers were placed into an oscillation light incubator (ZDX-150; Changzhou NUOJI instrument Co., Ltd, China) accompanied with continuous shake at 40 times per min during the exposure process to ensure even distribution of MC-LR in the exposure medium. The incubation temperature was 26.0 ± 0.5°C under a 12-h light/12-h dark photoperiod. The nominal concentrations of MC-LR were 16, 32, 64, 128, 256, 512, and 1024 μmol/l. The control was cultured in the reconstituted buffer (ISO 6341). Photographs indicating the toxic effects on embryos and larvae were obtained from 1 to 15 days post fertilization with an inverted microscope (TE2000-U). Death was defined by cessation of heartbeat or coagulation of the embryos. Dead embryos and larvae were removed promptly from the petri dishes, and the mortalities of embryos and larvae were calculated. The LC_{50} for the embryos and larvae were calculated by probit analysis. Each test was replicated three times.

RESULTS AND DISCUSSION

Interactions between MC-LR and SML

Lecithin is ubiquitous in cells and is a component of the cell membrane phospholipid bilayer. SML, prepared by dispersing lecithin in water, is used to simulate the phospholipid membrane (Li *et al.*, 2007). In the SML/MC-LR reaction liquid, the equilibrium concentration (c_e) of MC-LR was determined using HPLC-DAD (see Supplementary 2, Fig. S1). The association of MC-LR with SML approached equilibrium after approximately 4 h (see Supplementary 2, Fig. S3A). As Figure 1 demonstrates, the amount of MC-LR adsorbed (q_e) approached equilibrium with an increase in c_e to 2.0 mmol/l. The q_e increased linearly with an increase in c_e from 2.0 to 3.0 mmol/l. These data were fitted to different models to elucidate the interaction between MC-LR and SML (see Supplementary 2, Fig. S4). The q_e increased and approached a constant maximum at the initial concentration (c_0) of 2.2 mmol/l (see Supplementary 2, Fig. S4A). The $-NH_3^+$ and $-COO^-$ groups of MC-LR may bind to the $>PO_4^-$ and $N(CH_3)_3^+$ groups of PC, respectively, through ion-pair attraction and hydrogen bonding (Fig. 1b). The interaction is similar to that of the aggregation of amphoteric compounds on amphoteric surfactant micelles (Soontravanich *et al.*, 2008; Wang *et al.*, 2006), which obeys the Langmuir isotherm model (Langmuir, 1918). Therefore, the data presented in Supplementary Figure S4A were fitted to the Langmuir isothermal equation (see Supplementary 1, Equation S1). In view of the good linearity, the binding of MC-LR to SML obeyed the monolayer adsorption when c_e ranged between 0.014 and 2.0 mmol/l (Fig. 1a-1). From the regression

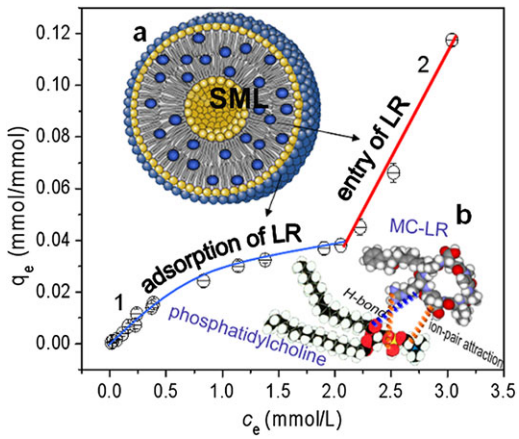

FIG. 1. The change in the bound amount (q_e) of MC-LR on SML (4.0 mmol/l PC) with an increase in the equilibrium concentration (c_e) from 0.01 to 3.0 mmol/l in MC-LR/SML solutions for 4 h incubation. ''1'' Stands for the MC-LR absorption on the outer surface of SML; ''2'' stands for the MC-LR distribution inside of SML; ''a'' presents the model for MC-LR distribution in different parts of SML; ''b'' demonstrates the interaction mode between MC-LR and SML.

plots concerning q_e^{-1} versus c_e^{-1}, a slope ($1/NK$) and intercept ($1/N$) were calculated (see Supplementary 2, Fig. S4A). The saturation adsorption mole number (N) of MC-LR was 0.038 ± 0.003 moles per mole of PC, that is, one MC-LR molecule bound to approximately 26 PC molecules. The binding constant (K) was (1.05 ± 0.05) × 10^3 l/mol. However, when c_0 exceeded 2.2 mmol/l, there was a linear increase in MC-LR binding to SML (see Supplementary 2, Fig. S4B). From plots concerning q_e versus c_e (see Supplementary 2, Fig. S4B), the binding of MC-LR to SML fitted the Pesavento partition model (Leo *et al.*, 1971). The partition constant ($P_{PC} = q_e/c_e$) (see Supplementary 1, Equation S2) was 117.4 l/kg, that is, log P = 2.07. MC-LR is hydrophobic (log P_{ow} = 4.2) (Rivasseau *et al.*, 1998) as it contains a hydrophobic phenyl moiety (see Supplementary 2, Fig. S1). Therefore, it may enter the long aliphatic chain region of PC in SML by hydrophobic effects (Fig. 1a-2). Although it is hydrophobic, MC-LR possesses some polar entities including carboxylic acids, amino, and amido groups (see Supplementary 2, Fig. S1) and demonstrates hydrophilic and hydrophobic functions. SML formed from the bipolar PC molecule have strong polarity in the outer shell, interacting with hydrophilic phosphoric acid and amino groups, but demonstrate strong hydrophobic properties internally, interacting with the long hydrophobic aliphatic chain of PC. Therefore, low concentrations of MC-LR confronted with the polar surface of SML would adsorb on to SML via its polar functions. With an increase in MC-LR concentration, it would be transported through the hydrophilic surface and accumulate between the hydrophobic region and the long aliphatic chain through hydrophobic interactions, after adsorption saturation had been reached on the outer surface of SML.

Effects of Electrolyte, pH, and Temperature on MC-LR/SML Interactions

The q_e decreased markedly with an increase in ionic strength to 0.15 mol/l (Fig. 2A). Much Cl^- was adsorbed on to the zwitterionic head group dipoles (Petrache *et al.*, 2006; Ulrich, 2002) to form anion layers. As the screening of Cl^- ions increased, so did the electrostatic repulsion with $-COO^-$ of MC-LR, which does not favor close interaction between MC-LR and SML. However, an increase in ionic strength decreases the activity coefficient of the solvent, driving MC-LR to partition into the hydrophobic inner layer of SML. Thus, q_e increased at an ionic strength > 0.15 mol/l (Fig. 2A); it decreased within the pH range 2.5–7.5 (Fig. 2B). The pK_a of PC is approximately 0.8 (Moncelli *et al.*, 1994), and the $>PO_4^-$ ions of SML predominate within this pH range. MC-LR has two carboxylic groups on its glutamic and aspartic acid side chains and one guanidine group residing on the arginine side chain. In an acidic medium, the amino group (NH_3^+) of the guanidine moiety and the g-carboxylic group (-COOH) are protonated, so in MC-LR has a positive overall charge. The ion-pairs occurred between $>PO_4^-$ groups in PC of SML and the positively charged NH_3^+ group on the guanidine group of arginine residues in MC-LR. Therefore, q_e was higher in a very acidic medium (pH = 2.5). The dissociation of carboxylic groups occurs around pH 3.3–3.4 (Rivasseau *et al.*, 1998), and the carboxylic entities evolve into their carboxylate form $-COO^-$ at a pH higher than 3.5. MC-LR gradually changed from an ampholitic form to one that was neutral and then to one with an anionic overall charge. In basic medium, the guanidine residue became neutral ($-NH_2$) and MC-LR possessed two negative charges owing to the g-COO^- groups. The decrease in q_e can be explained by the ionization of these two carboxylic groups at a pH higher than 3.5. This makes MC-LR amphoteric or negatively charged, which is not favorable for MC-LR binding to SML owing to electrostatic repulsion; therefore, q_e decreased with increasing pH (Fig. 2B). The q_e increased with an increase in temperature (Fig. 2C). The plots of ln$K$ versus T^{-1} fitted the van't Hoff equation (see Supplementary 1, Equation S3; Rombough, 1985). The entropy change (ΔS) was calculated as 89.8 ± 0.8 J/mol/K and the enthalpy change (ΔH) as +9.8 ± 0.3 kJ/mol. The free enthalpy ($\Delta G = \Delta H - T\Delta S$) was calculated as −19.59 ± 0.03 to −15.99 ± 0.02 kJ/mol within the temperature range examined (see Supplementary 2, Fig. S5). The MC-LR/SML interaction is spontaneous and driven by entropy increases. The endothermic reaction indicated that a higher temperature favored MC-LR binding to SML.

Association of MC-LR with Embryos

Ten embryos were exposed to MC-LR to investigate the interaction between them. MC-LR adsorption on embryos reached equilibrium at approximately 36 h (see Supplementary 2, Fig. S3B), which is longer than that experienced *in vitro* (see

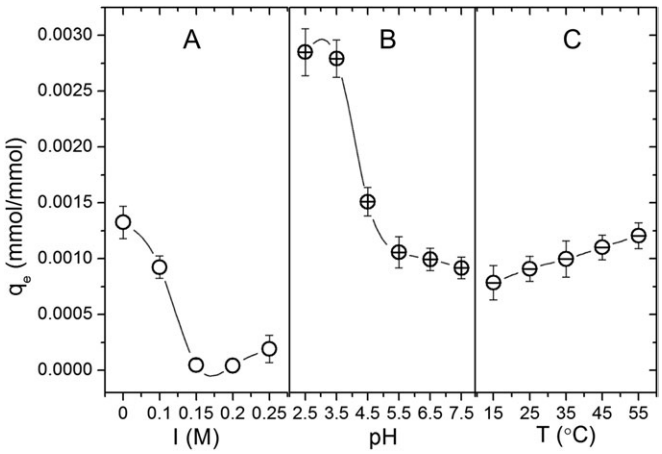

FIG. 2. Effects of ionic strength (A), pH (B), and temperature (°C) on q_e of MC-LR (the initial exposure concentration, c_0, 0.03 mmol/l) on SML (4.0 mmol/l PC) after 4 h incubation.

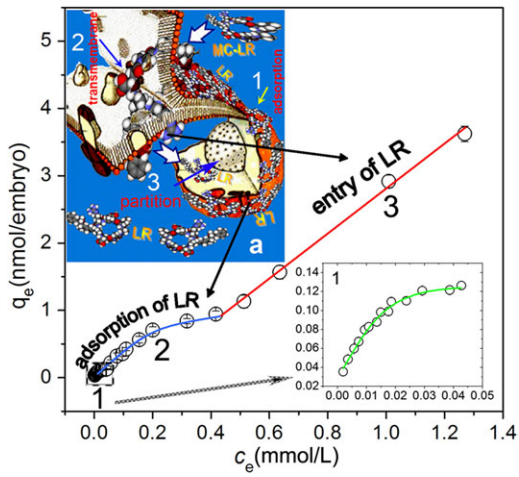

FIG. 3. The change in q_e of MC-LR on zebrafish embryos ($n = 10$) with an increase in c_e from 0.004 to 1.3 mmol/l in MC-LR solutions after 36 h exposure. ''1'' Stands for the Langmuir absorption stage for MC-LR on the outer membrane surface, ''2'' stands for the Freundlich absorption stage for MC-LR both on outside of membrane and inside of the membrane phospholipid bilayer, and ''3'' stands for the partition stage of MC-LR from the membrane to the cytoplasm of embryos; ''a-1'' demonstrates MC-LR adsorption on the outer membrane surface, ''a-2'' demonstrates MC-LR transmembrane transport from the outer membrane surface to inside the membrane phospholipid bilayer, and ''a-3'' demonstrates MC-LR partition from the membrane phospholipid bilayer to the cytoplasm.

Supplementary 2, Fig. S3A). The main reason for this is that MC-LR is less accessible to the embryo than to SML. In addition, the barrier role of the embryonic membrane and the growth and metabolism of the embryo affect the transport of MC-LR. As in the *in vitro* experiments, the change in q_e on embryos was apparent during the absorption and partition stages: q_e demonstrated two consecutive absorption process at low c_e of MC-LR (Fig. 3-1 and 3-2) and q_e increased linearly when c_e was > 0.4 mmol/l (Fig. 3-3). To understand the adsorption characteristics of MC-LR on embryos better, various models were used to fit the q_e data for different concentrations of MC-LR (see Supplementary 2, Fig. S6). q_e approached a maximum when c_0 was increased to 0.04 mmol/l (see Supplementary 2 Fig S6A). The data conformed to the Langmuir adsorption isotherm (see Supplementary 1, Equation S1). From plots of q_e^{-1} versus c_e^{-1} (see Supplementary 2, Fig. S6A), N of MC-LR on embryos was calculated as 0.13 ± 0.006, that is, 0.13 nmole of MC-LR bound to one embryo. K was calculated as $(1.73 \pm 0.004) \times 10^5$ l/mol, which is higher than that obtained *in vitro* using SML. Therefore, MC-LR was distributed more readily on the embryo membranes, probably facilitated by functional groups such as carboxyl, amino, sulfate, phosphate, amide, and hydroxyl imidazole (Bhainsa and D'Souza, 2008; Yan and Viraraghavan, 2003). The q_e tended to be balanced when c_0 was 0.40 mmol/l (see Supplementary 2, Fig S6B). This adsorption process followed the Freundlich isotherm model (see Supplementary 1, Equation S4; Nounou and Nounou, 2010) from 0.05 to 0.4 mmol/l. From plots of log q_e versus log c_e (see Supplementary 2, Fig. S6B), the heterogeneity factor ($1/n$) was calculated as 0.73 ± 0.05, demonstrating that MC-LR was not only adsorbed on to the outer membrane surface but distributed inside the membrane phospholipid bilayer and in the cytoplasm. When c_0 was > 0.5 mmol/l, q_e increased linearly with an increase in c_0 (see Supplementary 2, Fig. S6C). The association with MC-LR conformed to a general partition model (see Supplementary 1, Equation S2). The partition coefficient (P_{embryo}) was calculated as 3.34 ± 0.14 ml per embryo (see Supplementary 2, Fig. S6C), that is, approximately 113 l/kg, approaching that obtained *in vitro* using SML.

Ionic strength, pH, and temperature affected the binding of MC-LR to embryos (see Supplementary 2, Fig. S7). As with the SMLs, q_e on embryos decreased with increased ionic strength (see Supplementary 2, Fig. S7A) as large amounts of Cl^- tended to adsorb to the outer membrane surface (Petrache *et al.*, 2006; Ulrich, 2002), and this is not favorable for the binding of MC-LR to the membrane. The q_e decreased when the pH was > 3.5 (see Supplementary 2, Fig. S7B). A possible reason is that the carboxylic groups of MC-LR evolved into their carboxylate form -COO^- (Rivasseau *et al.*, 1998), which does not favor binding of MC-LR to embryos. The q_e increased with increased temperature (see Supplementary Fig. S7C). The difference between q_e on embryos and SMLs is that q_e increased at an ionic strength of 0.1 mmol/l and a pH of 7.4. These ionic strength and pH conditions were close to normal conditions favorable for the physiological activity of embryos (see Supplementary 2, Figs. S7A and 7B). The q_e decreased when the temperature was > 40°C, but this affected embryonic activity (see Supplementary 2, Fig. S7C).

Membrane Distribution of MC-LR

The membrane, which consists of a phospholipid bilayer, membrane proteins, and oligosaccharides, acts as a natural

barrier and plays a protective role during normal cellular activity. It performs a number of essential functions including nutrient transport, ion conduction, and signal transduction. Accumulation of harmful chemicals in the membrane may cause membrane expansion, blockage of ion pumps and altered proton permeability (Panda *et al.*, 1999; Saar *et al.*, 2005; Sikkema *et al.*, 1994). Understanding transmembrane transport of chemicals is useful for understanding their underlying toxicity mechanisms. The distribution of MC-LR among various parts of the embryos was determined by fragmenting the embryos and examining MC-LR levels (see Supplementary 2, Fig. S2). The majority of the MC-LR remained in the extracellular medium (Fig. 4). When c_0 was < 0.044 mmol/l, > 75% of the adsorbed MC-LR was located on the outer membrane surface and less than 6% entered the cytoplasm (see Supplementary 2, Fig. S8), that is, more than 0.099 nmole was present on the outer membrane surface and 0.006 nmole entered the cytoplasm of one embryo (Fig. 4A). At MC-LR concentrations of 0.06 to 0.50 mmol/l, the adsorbed MC-LR was predominantly distributed inside the membrane phospholipid bilayer, with some evident in the cytoplasm; q_e in these two fractions increased in line with an increase in c_0 (Fig. 4B). However, the percentage distribution of MC-LR inside the membrane decreased, whereas that in the cytoplasm gradually increased. The percentages in these two fractions were comparable when c_0 increased to 0.50 mmol/l (see Supplementary 2, Fig. S8), demonstrating that MC-LR was continuously transported from the membrane to the cytoplasm until equilibrium was reached. At a concentration > 0.5 mmol/l, q_e in the cytoplasm increased with an increase in c_0 (Fig. 4C). When c_0 was > 1.0 mmol/l, over 70% of the adsorbed MC-LR was distributed in the cytoplasm, < 5% on the outer membrane surface, and > 23% inside the membrane (see Supplementary 2, Fig. S8), that is, more than 2.13 nmole of MC-LR were transported into the cytoplasm but only 0.65 nmole inside the membrane and 0.13 nmole on the outer membrane surface (Fig. 4C). The data demonstrate that different concentrations of MC-LR cause alterations in membrane distribution (Figs. 4A–C) and may represent different membrane transport processes involved in delivering MC-LR from the extraembryonic medium to the developing embryonic cells. A scheme of the possible membrane transport processes included three stages (Fig. 4D): (1) surface adsorption, (2) transmembrane transport, and (3) intracellular accumulation.

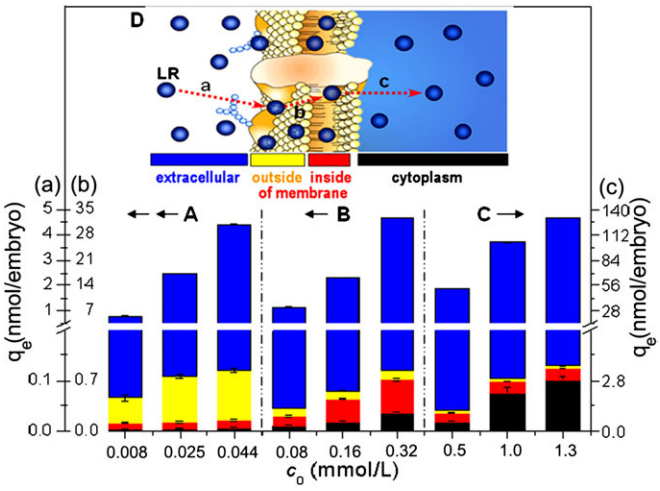

FIG. 4. The distribution of various concentrations of MC-LR (A, B, C) in different parts (extracellular fluid, outside and inside of membrane and cytoplasm) of embryos (n = 10) after 36 h exposure, and the illustration of transmembrane transport process (D) for MC-LR from the extracellular fluid to the cytoplasm of embryos: (A) the lower concentrations of MC-LR (c_0: 0.008, 0.025, and 0.044 mmol/l); (B) the intermediate concentrations of MC-LR (c_0: 0.08, 0.16, and 0.32 mmol/l); (C) the higher concentrations of MC-LR (c_0: 0.5, 1.0, and 1.3 mmol/l); (D) the membrane transport process of MC-LR (a, from extracellular fluid to outer membrane surface; b, from outer membrane surface to inside the membrane phospholipid bilayer; c, from inside the membrane phospholipid bilayer to the cytoplasm).

Diffusion Dynamic Model

The adsorption of MC-LR on to embryos (Fig. 3) and its distribution among various parts of the embryo (Fig. 4) were studied. Initially, the membrane surface was free from MC-LR, and when MC-LR reached the surface, it may have instantly attached to the binding sites. Therefore, the adsorption rate could be dominated by the number of MC-LR molecules diffusing from the extra-embryonic solution to the embryonic surface. This implies that the adsorption process can be analyzed by diffusion-controlled dynamics (McKay and Poots, 1980), presented as:

$$q_t = 2c_0 S\sqrt{Dt/\pi} = k_d t^{0.5}, \quad (1)$$

Where q_t (nmol/embryo) represents the amount of MC-LR adsorbed on one embryo at time "t," c_0 is the initial exposure concentration of MC-LR in solution, D is the diffusion coefficient, and S is the specific surface area of the embryonic membrane (Das *et al.*, 2006). According to the adsorption kinetics data in Figure 5A, the regression plots concerning q_t versus $t^{0.5}$ was shown in Figure 5B. Therefore, the plot of q_t versus $t^{0.5}$ would be a straight line under a diffusion-controlled transport mechanism. The results presented in Figure 5B demonstrate different characteristics for various concentrations of MC-LR but appear linear at 0.03 mmol/l (Fig. 5B-1) and 1.3 mmol/l (Fig. 5B-3), demonstrating that the adsorption process at these two concentrations obeys the diffusion-controlled dynamics model (Equation 1). At low concentrations, MC-LR was adsorbed to the outer membrane surface directly from the extracellular fluid (Fig. 5B-1) and partitioned freely through the membrane into the cytoplasm at high concentrations (Fig. 5B-3). The transport process demonstrated a multilinearity of three stages at a concentration of 0.3 mmol/l (Fig. 5B-2). In this concentration, the adsorption data for MC-LR did not obey the diffusion-controlled dynamics model, that is, (1) the initial sharp portion can be attributed to the

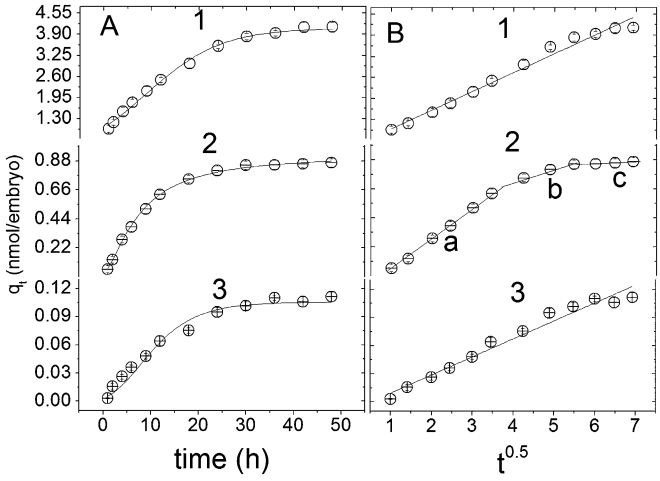

FIG. 5. Diffusion control kinetic model for various concentrations of MC-LR (from 1 to 3, 0.03, 0.30, and 1.30 mmol/l) on embryos ($n = 10$); 2-a, adsorption stage; 2-b, transport stage; and 2-c, partition stage.

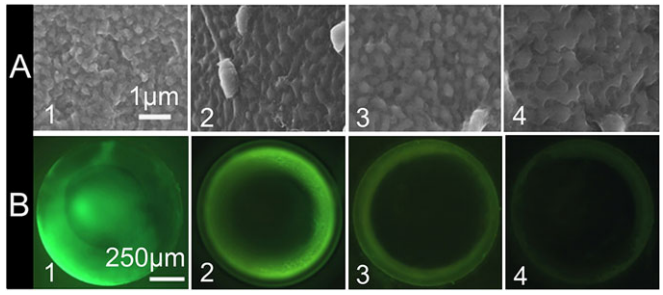

FIG. 6. SEM and fluorescent morphology observations of the embryo membrane after the embryos ($n = 10$) were exposed to various concentrations of MC-LR (from 1 to 4, 0, 0.01, 0.1, and 1.0 mmol/l) for 12 h. (A) SEM morphology observed with scanning electron microscopy. (B) Fluorescent morphology observed with the inverted fluorescence microscope.

instantaneous adsorption at the outer membrane surface; (2) the gradual adsorption is controlled by the transfer rate of MC-LR from the outer membrane surface to inside the membrane phospholipid bilayer; and (3) the third stage is the final partition where the rate is controlled by the different partition coefficients for MC-LR in the membrane and cytoplasm. Therefore, the three-stage results from dynamics (Fig. 5) are consistent with the results concerning the adsorption of MC-LR on to the embryo (Fig. 3, see Supplementary 2, Fig. S6) and the distribution process governing MC-LR expression in various parts of the embryo (Fig. 4).

Transmembrane Transport Mechanism

The embryonic membrane contains several hydrophilic groups such as carboxyl, amino, sulfate, phosphate, amide, and hydroxyl imidazole (Bhainsa and D'Souza, 2008; Yan and Viraraghavan, 2003). Therefore, many polar groups including -COOH, -OH, and -NH_2 are distributed on the outer membrane surface. MC-LR contains several hydrophilic groups including carboxylic acid and guanidine residues (see Supplementary 2, Fig. S1), has strong polarity, and is water soluble. Therefore, the polar groups of MC-LR and those present in the embryonic membrane would interact in solution. The initial attachment of MC-LR to embryonic membrane surfaces is due to: (1) electrostatic interaction between the polar groups of MC-LR and the electron-rich sites on the embryonic membrane surface and (2) weak physical forces such as hydrogen bonds and van der Waals interactions between the hydrophobic portions (the aromatic rings) of MC-LR and the polysaccharides of the embryonic membrane (Blackburn, 2004). MC-LR was adsorbed on to the outer membrane surface via ion-pair attraction, hydrogen bonds, and van der Waals forces (Fig. 3a-1). In addition, polar organic chemicals exert transmembrane impedance effects (TMIE) (Ren *et al.*, 2010). In low concentrations of MC-LR, there was evidence of TMIE. The combination of various interactions between MC-LR and embryos and the TMIE caused low concentrations of MC-LR to adsorb firmly to the outer membrane surface. SEM analysis and the morphology of membranes observed after fluorescence microscopy confirmed that low concentrations of MC-LR were predominantly adsorbed on the outer membrane surface and caused the membrane layer to become obscured (Fig. 6A-2), resulting in decreased fluorescence intensity (Fig. 6A-2).

After surface adsorption, MC-LR was transported from the outer membrane surface into the membrane phospholipid bilayer (Fig. 3a-2), owing to the scarcity of available binding sites on the outer membrane surface and the high hydrophobic action of MC-LR (Rivasseau *et al.*, 1998). Results relating to adsorption (see Supplementary 2, Fig. S6B), distribution (Fig. 4B), and dynamics (Fig. 5B-2) indicated that MC-LR was adsorbed on to the outer membrane and inside the membrane phospholipid bilayer at a concentration range of 0.05 to 0.4 mmol/l. Furthermore, fluorescence intensity outside and inside the membrane (Fig. 6B-3) was lower than in the control (Fig. 6B-1).

High concentrations of MC-LR resulted in the membrane surface becoming flat and the average spacing of polar heads of phospholipids increased (Fig.6A-4) thinning the membrane (van Rooijen *et al.*, 2009), and this was confirmed by fluorescence analysis: the fluorescence intensity decreased and the fluorescent layer was thinner when high concentrations of MC-LR were employed (Fig. 6B-4). Membrane thinning has been suggested as a possible mode of membrane disruption (Sokolov *et al.*, 2006). The distribution of MC-LR in various parts of embryos was related to different partition coefficients (Vanwezel and Opperhuizen, 1995). As the partition coefficients of MC-LR in storage lipids are higher than in phospholipids, MC-LR was readily partitioned from membrane phospholipids to the cytoplasm, which contains many storage lipids (Fig. 3a-3). The highly lipophilic MC-LR could move easily through the thinned and disrupted membrane to accumulate in the cytoplasm and caused acute death within 36 h (see Supplementary 2, Fig. S9).

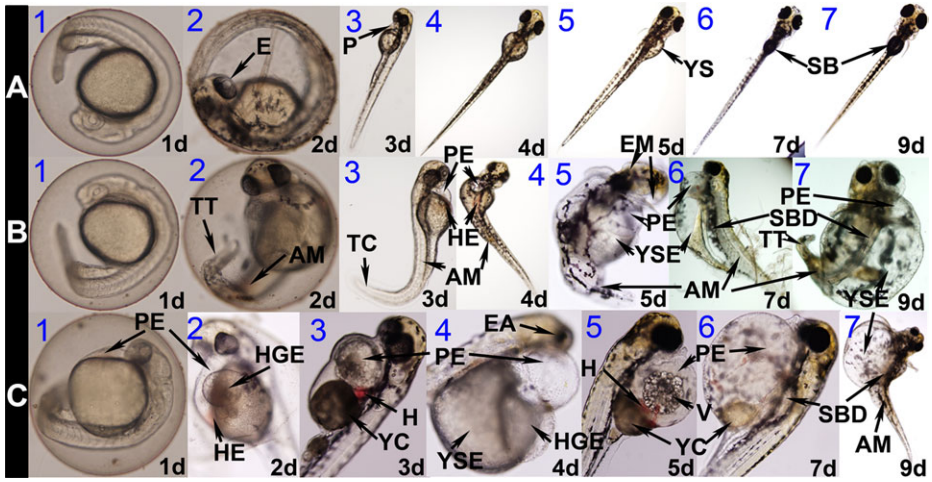

FIG. 7. MC-LR exposure induced various developmental defects in embryos and larvae. (A) Control groups demonstrated normal development in reconstituted buffer; (B) 0.01 mmol/l MC-LR exposure groups; (C) 0.1 mmol/l MC-LR exposure groups. E, eye; EA, eye abnormalities; EM, eye missing; P, pericardial; SB, swim bladder; YC, yolk condensation, YS, yolk sac.

The results relating to absorption, distribution, kinetics, SEM, and fluorescence demonstrated that different concentrations of MC-LR behaved differently in terms of transmembrane transport processes, and the possible mechanisms are (1) diffusion from the extracellular medium to the outer membrane surface and adsorption by electrostatic attraction, hydrogen bonds, and van der Waals forces (Figs. 3a-1 and 4D-a); (2) transmembrane transport from the outer membrane surface into the membrane phospholipid bilayer owing to the high lipophilicity of MC-LR and the activity and metabolism of embryos (Figs. 3a-2 and 4D-b); (3) partition from the membrane phospholipid bilayer to the cytoplasm owing to the different partition coefficients between the phospholipid bilayer and storage lipids (Figs. 3a-3 and 4D-c).

Effects of MC-LR on the Development of Zebrafish Embryos and Larvae

Photographs taken during zebrafish embryo development demonstrated normal development in control embryos and larvae (Fig. 7A), whereas those exposed to various concentrations of MC-LR had different degrees of deformity (Figs. 7B and 7C). Exposure to a low concentration of 0.01 mmol/l MC-LR showed normal development for 1-day exposure, but embryos showed obvious tail twisting (TT) and axial malformation (AM) for 2 days exposure (Fig. 7B-2). The larvae showed slight pericardial edema (PE) and hemagglutination (HE) for 3 days exposure (Fig. 7B-3) and obvious PE, yolk sac edema (YSE), and swim bladder defect after 5 days exposure (Fig. 7B-5,6,7). At a concentration of 0.1 mmol/l MC-LR, embryos showed obvious pericardial edema (PE) just for 1-day exposure (Fig. 7C-1) and serious HE and hatching gland edema (HGE) for 2 days exposure (Fig. 7C-2). The larvae presented with very serious PE, hemorrhage (H), and yolk condensation for 3 days exposure (Fig. 7C-3) and extraordinary severe vacuolization (V) in the pericardium for 5 days exposure (Fig. 7C-5).

Figure 8 presents the mortality of embryos and larvae after long-term exposure to different concentrations of MC-LR. Acute lethal toxicity was apparent in 256 μmol/l MC-LR exposure groups with all embryos dying within 3 days, and chronic sublethal toxicity was evident in groups exposed to < 128 μmol/l with only 30% dying after 5 days exposure to 128 μmol/l MC-LR (Fig. 8A). In contrast, it took 6 days for all larvae to die in the group exposed to 256 μmol/l MC-LR, whereas only 20% died after 7 days exposure to 128 μmol/l (Fig. 8B). The median lethal concentration (LC_{50}) of MC-LR was calculated from the mortality date for embryos and larvae. The 2-day LC_{50} was approximately 273 μmol/l for embryos and 724 μmol/l for larvae, whereas the 8-day LC_{50} were 78 μmol/l for embryos and 72 μmol/l for larvae. Therefore, the embryos were more sensitive to the high concentration of MC-LR than larvae, but the converse was true for exposure to the low concentration. This supports the view that the low

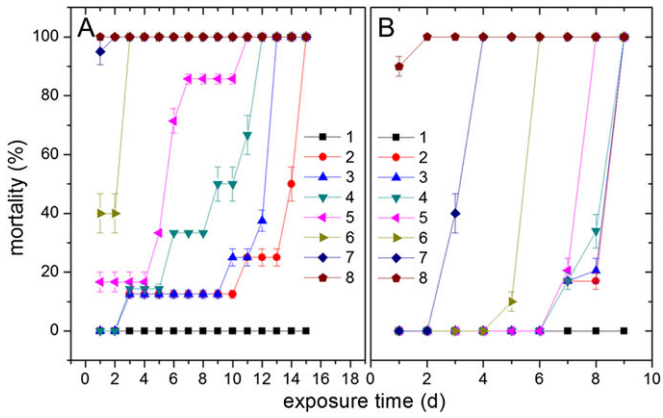

FIG. 8. Mortality of embryos (A) and larvae (B) exposed to various concentrations of MC-LR (from 1 to 8, 0, 16, 32, 64, 128, 256, 512, and 1024 μmol/l) for different time to evaluate the acute and chronic lethal toxicities.

concentration of MC-LR was predominantly adsorbed to the outer membrane surface (Fig. 4A), which did not result in embryonic death at a concentration < 64 μmol/l (Fig. 8A) owing to the protective function of the membrane.

The toxic characteristics caused by different concentrations of MC-LR are closely related to their different membrane transport processes. At concentrations < 64 μmol/l, adsorption on the outer membrane surface was predominant (Fig. 4A) which caused the membrane layer to become obscured (Fig. 6A-2). Although this binding of MC-LR on the outer membrane surface did not result in embryonic death (Fig. 8A), it altered the membrane structure, which may have affected the flow/rotation of phospholipids, transport of membrane proteins, and the import of necessary substances, resulting in TT, tail curving (TC), and AM (Fig. 7B). MC-LR is strong hydrophobic (Rivasseau *et al*., 1998) and was able to move from the outer membrane surface to the cytoplasm (Figs. 3a-2 and 4B) where it may have bound some proteins including bovine serum albumin, lysozyme, flavodoxin, myoglobin, and ferredoxin-$NADP^+$ reductase (Vela *et al*., 2008), affecting metabolism and causing chemical damage such as inhibition of serine/threonine protein phosphatases PP1 and PP2A (Hastie *et al*., 2005). This could result in promotion of tumors (Ohta *et al*., 1992), DNA damage (Zegura *et al*., 2008), disruption of oxidative phosphorylation (La-Salete *et al*., 2008), reduction of the myofibril volume fraction, and myocardial contractility (Milutnovic *et al*., 2006), leading to ventricular dysfunction and serious PE, YSE, and HGE and severe HE, H, and V in the pericardia of exposed embryos and larvae (Fig. 7C). When the concentrations of MC-LR were > 0.5 mmol/l, the exposed embryo membrane became thinned and disrupted (Figs. 6A and 6B-4) and the TMIE collapsed. More than 70% of MC-LR accumulated in the cytoplasm (see Supplementary 2, Fig. S8) and caused acute death within 36 h (see Supplementary 2, Fig. S9).

CONCLUSIONS

By investigating the interactions of MC-LR with SML and Zebrafish embryos, we established the separation and instrumentation method of MC-LR from membrane and cytoplasm and proposed the adsorption mechanism of MC-LR on embryo and its transmembrane transport pathway. Based on the teratogenic and lethal toxicity of MC-LR to zebrafish embryos and larvae, the transmembrane distribution of MC-LR has demonstrated the close correlation among its interaction, transport, and toxicity effects. MC-LR exhibited the different interaction way with embryos when it was exposed in the low and high concentration levels. MC-LR in low concentration exposure, for example, less than 0.04 mmol/l was absorbed mostly on outer surface of embryos by electrostatic attraction, hydrogen bond, and van der Waals force according to Langmuir isotherm and then caused the physical damage of embryos including TT, TC, and AM. When MC-LR is between 0.05 and 0.4 mmol/l, it transferred from outside membrane surface into membrane phospholipid bilayer fitting to Freundlich isotherm model and bound by the hydrophobic interaction and then caused the chemical damage and serious deformities of embryos including PE, YSE, HGE, HE, H, and V. When the exposure concentration of MC-LR is more than 0.5 mmol/l, it entered cytoplasm from membrane according to the water-lipid partition law and then caused the acute death of embryos. In addition, the SEM of embryo surface, fluorescence-probing observation of the embryo, and the adsorption kinetics of MC-LR in various exposure concentrations further confirmed the above accumulation and transport of MC-LR in/to embryo.

SUPPLEMENTARY DATA

Supplementary data are available online at http://toxsci.oxfordjournals.org/.

FUNDING

The Key Project of the State Key Laboratory of Pollution Control and Resource Reuse (from 2011 to 2014); The Ministry of Science and Technology of PRC; The National S&T Major Project of China (2008ZX07421-002); Key Laboratory Foundation of Education Ministry of China (YRWEY 1008).

ACKNOWLEDGMENT

Conflict of interest: The authors declare no competing financial interests.

REFERENCES

Bhainsa, K. C., and D'Souza, S. F. (2008). Removal of copper ions by the filamentous fungus, *Rhizopus oryzae* from aqueous solution. *Bioresource Technol*. **99,** 3829–3835.

Blackburn, R. S. (2004). Natural polysaccharides and their interactions with dye molecules: applications in effluent treatment. *Environ. Sci. Technol*. **38,** 4905–4909.

Das, S. K., Bhowal, J., Das, A. R., and Guha, A. K. (2006). Adsorption behavior of rhodamine B on *Rhizopus oryzae* biomass. *Langmuir* **22,** 7265–7272.

Djediat, C., Malecot, M., de Luze, A., Bernard, C., Puiseux-Dao, S., and Edery, M. (2010). Localization of microcystin-LR in medaka fish tissues after cyanotoxin gavage. *Toxicon* **55,** 531–535.

Donato, M. M., Jurado, A. S., Antunes-Madeira, M. C., and Madeira, V. M. C. (1997a). Effects of a lipophilic environmental pollutant (DDT) on the phospholipid and fatty acid contents of Bacillus stearothermophilus. *Arch. Environ. Contamin. Toxicol*. **33,** 341–349.

Donato, M. M., Jurado, A. S., Antunes-Madeira, M. C., and Madeira, V. M. C. (1997b). Bacillus stearothermophilus as a model to evaluate membrane toxicity of a lipophilic environmental pollutant (DDT). *Arch. Environ. Contamin. Toxicol*. **33,** 109–116.

Fastner, J., Codd, G. A., Metcalf, J. S., Woitke, P., Wiedner, C., and Utkilen, H. (2002). An international intercomparison exercise for the determination of purified microcystin-LR and microcystins in cyanobacterial field material. *Anal. Bioanal. Chem.* **374,** 437–444.

Fei, X. C., Song, C., and Gao, H. W. (2010). Transmembrane transports of acrylamide and bisphenol A and effects on development of zebrafish (*Danio rerio*). *J. Hazard. Mater.* **184,** 81–88.

Fischer, W. J., and Dietrich, D. R. (2000). Toxicity of the cyanobacterial cyclic heptapeptide toxins microcystin-LR and -RR in early life-stages of the African clawed frog (*Xenopus laevis*). *Aquat. Toxicol.* **49,** 189–198.

Gan, N., Sun, X., and Song, L. (2010). Activation of Nrf2 by microcystin-LR provides advantages for liver cancer cell growth. *Chem. Res. Toxicol.* **23,** 1477–1484.

Hastie, C. J., Borthwick, E. B., Morrison, L. F., Codd, G. A., and Cohen, P. T. (2005). Inhibition of several protein phosphatases by a non-covalently interacting microcystin and a novel cyanobacterial peptide, nostocyclin. *Biochim. Biophys. Acta* **1726,** 187–193.

Herfindal, L., and Selheim, F. (2006). Microcystin produces disparate effects on liver cells in a dose dependent manner. *Mini-Rev. Med. Chem.* **6,** 279–285.

Huynh-Delerme, C., Edery, M., Huet, H., Puiseux-Dao, S., Bernard, C., Fontaine, J. J., Crespeau, F., and de Luze, A. (2005). Microcystin-LR and embryo-larval development of medaka fish, *Oryzias latipes*. I. Effects on the digestive tract and associated systems. *Toxicon* **46,** 16–23.

Jacquet, C., Thermes, V., de Luze, A., Puiseux-Dao, S., Bernard, C., Joly, J. S., Bourrat, F., and Edery, M. (2004). Effects of microcystin-LR on development of medaka fish embryos (*Oryzias latipes*). *Toxicon* **43,** 141–147.

Jayaraj, R., Anand, T., and Rao, P. V. L. (2006). Activity and gene expression profile of certain antioxidant enzymes to microcystin-LR induced oxidative stress in mice. *Toxicology* **220,** 136–146.

La-Salete, R., Oliveira, M. M., Palmeira, C. A., Almeida, J., and Peixoto, F. P. (2008). Mitochondria a key role in microcystin-LR kidney intoxication. *J. Appl. Toxicol.* **28,** 55–62.

Lahnsteiner, F. (2008). The sensitivity and reproducibility of the zebrafish (*Danio rerio*) embryo test for the screening of waste water quality and for testing the toxicity of chemicals. *Altern. Lab. Anim.* **36,** 299–311.

Langmuir, I. (1918). The adsorption of gases on plane surfaces of glass, mica and platinum. *J. AM. Chem. Soc.* **40,** 1361–1403.

Leo, A., Hansch, C., and Elkins, D. (1971). Partition coefficients and their uses. *Chem. Rev.* **71,** 525–616.

Li, H. Y., Xie, P., Zhang, D. W., and Chen, J. (2009). The first study on the effects of microcystin-RR on gene expression profiles of antioxidant enzymes and heat shock protein-70 in *Synechocystis sp* PCC6803. *Toxicon* **53,** 595–601.

Li, L., Gao, H. W., Ren, J. R., Chen, L., Li, Y. C., Zhao, J. F., Zhao, H. P., and Yuan, Y. (2007). Binding of Sudan II and IV to lecithin liposomes and E-coli membranes: insights into the toxicity of hydrophobic azo dyes. *BMC Struct. Biol.* **7,** 16.

Li, W. Y., Chen, F. F., and Wang, S. L. (2010). Binding of reactive brilliant red to human serum albumin: Insights into the molecular toxicity of sulfonic azo dyes. *Protein Peptide Lett.* **17,** 621–629.

Lopes, V. I. C. F., AntunesMadeira, M. C., and Madeira, V. M. C. (1997). Effects of methylparathion on membrane fluidity and its implications for the mechanisms of toxicity. *Toxicol. In Vitro* **11,** 337–345.

Malbrouck, C., Trausch, G., Devos, P., and Kestemont, P. (2004). Effect of microcystin-LR on protein phosphatase activity and glycogen content in isolated hepatocytes of fed and fasted juvenile goldfish *Carassius auratus* L. *Toxicon* **44,** 927–932.

Martins, J. D., Monteiro, J. P., Antunes-Madeira, M. C., Jurado, A. S., and Madeira, V. M. C. (2003). Use of the microorganism *Bacillus stearothermophilus* as a model to evaluate toxicity of the lipophilic environmental pollutant endosulfan. *Toxicol. In Vitro* **17,** 595–601.

McKay, G., and Poots, V. J. P. (1980). Kinetics and diffusion processes in color removal from effluent using wood as an adsorbent. *J. Chem. Technol. Biotechnol.* **30,** 279–292.

Mezhoud, K., Praseuth, D., Puiseux-Dao, S., Francois, J. C., Bernard, C., and Edery, M. (2008). Global quantitative analysis of protein expression and phosphorylation status in the liver of the medaka fish (*Oryzias latipes*) exposed to microcystin-LR I. Balneation study. *Aquat. Toxicol.* **86,** 166–175.

Miller, M. A., Kudela, R. M., Mekebri, A., Crane, D., Oates, S. C., Tinker, M. T., Staedler, M., Miller, W. A., Toy-Choutka, S., Dominik, C., *et al.* (2010). Evidence for a novel marine harmful algal bloom: cyanotoxin (microcystin) transfer from land to sea otters. *PLoS One.* **5,** e12576. Available at: http://www.plosone.org/article/info:doi/10.1371/journal.pone.0012576. Accessed June 7, 2011..

Milutnovic, A., Zorc-Pleskovic, R., Petrovic, D., Zorc, M., and Suput, D. (2006). Microcystin-LR induces alterations in heart muscle. *Folia Biol.* **52,** 116–118.

Moncelli, M. R., Becucci, L., and Guidelli, R. (1994). The Intrinsic Pk(a), values for phosphatidylcholine, phosphatidylethanolamine, and phosphatidylserine in monolayers deposited on mercury-electrodes. *Biophys. J.* **66,** 1969–1980.

Monteiro, J. P., Martins, J. D., Luxo, P. C., Jurado, A. S., and Madeira, V. M. C. (2003). Molecular mechanisms of the metabolite 4-hydroxytamoxifen of the anticancer drug tamoxifen: use of a model microorganism. *Toxicol. In Vitro* **17,** 629–634.

Nagel, R. (2002). DarT: the embryo test with the zebrafish *Danio rerio*—a general model in ecotoxicology and toxicology. *Altern. Tierexp.* **19,** 38–48.

Nounou, M. N., and Nounou, H. N. (2010). Multiscale estimation of the Freundlich adsorption isotherm. *Inter. J. Environ. Sci. Technol.* **7,** 509–518.

Ohta, T., Nishiwaki, R., Yatsunami, J., Komori, A., Suganuma, M., and Fujiki, H. (1992). Hyperphosphorylation of cytokeratins 8 and 18 by microcystin-LR, a new liver tumor promoter, in primary cultured rat hepatocytes. *Carcinogenesis* **13,** 2443–2447.

Panda, S. S., Mohapatra, P. K., and Mohanty, R. C. (1999). Comparative toxicity of two organophosphorus insecticides on membrane integrity of *Chlorella vulgaris*. I. Effect on membrane permeability. *Microbiol. Res.* **153,** 363–368.

Petrache, H. I., Zemb, T., Belloni, L., and Parsegian, V. A. (2006). Salt screening and specific ion adsorption determine neutral-lipid membrane interactions. *Proc. Natl. Acad. Ssi. U.S.A.* **103,** 7982–7987.

Ren, J. R., Zhao, H. P., Song, C., Wang, S. L., Li, L., Xu, Y. T., and Gao, H. W. (2010). Comparative transmembrane transports of four typical lipophilic organic chemicals. *Bioresource Technol.* **101,** 8632–8638.

Rivasseau, C., Martins, S., and Hennion, M. C. (1998). Determination of some physicochemical parameters of microcystins (cyanobacterial toxins) and trace level analysis in environmental samples using liquid chromatography. *J. Chromatogr. A* **799,** 155–169.

Rombough, P. J. (1985). The influence of the zona radiata on the toxicities of zinc, lead, mercury, copper and silver ions to embryos of steelhead trout *Salmo gairdneri*. *Comp. Biochem. Physiol. C* **82,** 115–117.

Saar, K., Lindgren, M., Hansen, M., Eiriksdottir, E., Jiang, Y., Rosenthal-Aizman, K., Sassian, M., and Langel, U. (2005). Cell-penetrating peptides: a comparative membrane toxicity study. *Anal. Biochem.* **345,** 55–65.

Schwarzenberger, A., Courts, C., and von Elert, E. (2009). Target gene approaches: gene expression in *Daphnia magna* exposed to predator-borne kairomones or to microcystin-producing and microcystin-free Microcystis aeruginosa. *BMC Genomics*, **10**.

Sikkema, J., Debont, J. A. M., and Poolman, B. (1994). Interactions of cyclic hydrocarbons with biological-membranes. *J. Biol. Chem.* **269,** 8022–8028.

Sikkema, J., Debont, J. A. M., and Poolman, B. (1995). Mechanisms of membrane toxicity of hydrocarbons. *Microbiol. Rev.* **59,** 201–222.

Sokolov, Y., Kozak, J. A., Kayed, R., Chanturiya, A., Glabe, C., and Hall, J. E. (2006). Soluble amyloid oligomers increase bilayer conductance by altering dielectric structure. *J. Gen. Physiol.* **128,** 637–647.

Song, C., Gao, N. Y., and Gao, H. W. (2010). Transmembrane distribution of kanamycin and chloramphenicol: insights into the cytotoxicity of antibacterial drugs. *Mol. Biosyst.* **6,** 1901–1910.

Soontravanich, S., Munoz, J. A., Scamehorn, J. F., Harwell, J. H., and Sabatini, D. A. (2008). Interaction between an anionic and an amphoteric surfactant. Part I: monomer-micelle equilibrium. *J. Surfactants Deterg.* **11,** 251–261.

Stone, D., and Bress, W. (2007). Addressing public health risks for cyanobacteria in recreational freshwaters: the Oregon and Vermont framework. *Integr. Environ. Assess. Manag.* **3,** 137–143.

Tachi, M., Imanishi, S. Y., and Harada, K. (2007). Phosphoprotein analysis for investigation of *in vivo* relationship between protein phosphatase inhibitory activities and acute hepatotoxicity of microcystin-LR. *Environ. Toxicol.* **22,** 620–629.

Ulrich, A. S. (2002). Biophysical aspects of using liposomes as delivery vehicles. *Bioscience Rep.* **22,** 129–150.

van Rooijen, B. D., Claessens, M. M. A. E., and Subramaniam, V. (2009). Lipid bilayer disruption by oligomeric alpha-synuclein depends on bilayer charge and accessibility of the hydrophobic core. *BBA-Biomembr* **1788,** 1271–1278.

Vanwezel, A. P., and Opperhuizen, A. (1995). Thermodynamics of partitioning of a series of chlorobenzenes to fish storage lipids, in comparison to partitioning to phospholipids. *Chemosphere* **31,** 3605–3615.

Vela, L., Sevilla, E., Gonzalez, C., Bes, M. T., Fillat, M. F., and Peleato, M. L. (2008). Exploring the interaction of microcystin-LR with proteins and DNA. *Toxicol. In Vitro* **22,** 1714–1718.

Wang, H. L., Chen, J. L., and Zhang, Q. X. (2006). Adsorption of an amphoteric aromatic compound (p-aminobenzoic acid) onto different polymeric adsorbents. *Adsorpt. Sci. Technol.* **24,** 17–28.

Wang, P. J., Chien, M. S., Wu, F. J., Chou, H. N., and Lee, S. J. (2005). Inhibition of embryonic development by microcystin-LR in zebrafish, *Danio Rerio*. *Toxicon* **45,** 303–308.

Yan, G. Y., and Viraraghavan, T. (2003). Heavy-metal removal from aqueous solution by fungus *Mucor rouxii*. *Water Res.* **37,** 4486–4496.

Zegura, B., Zajc, I., Lah, T. T., and Filipic, M. (2008). Patterns of microcystin-LR induced alteration of the expression of genes involved in response to DNA damage and apoptosis. *Toxicon* **51,** 615–623.

Zhang, Y. L., Zhang, X. A., Fei, X. C., Wang, S. L., and Gao, H. W. (2010). Binding of bisphenol A and acrylamide to BSA and DNA: insights into the comparative interactions of harmful chemicals with functional biomacromolecules. *J. Hazard. Mater.* **182,** 877–885.

Zhou, L., Yu, H., and Chen, K. (2002). Relationship between microcystin in drinking water and colorectal cancer. *Biomed. Environ. Sci.* **15,** 166–171.